

Hydrogen permeation of black oxide-treated and diamond-like carbon-coated bearing steels using high-pressure hydrogen gas

*Junichiro Yamabe^{1),4)}, Daiki Takagoshi²⁾, Hisao Matsunaga^{3),4)},
Hiroki Yamada⁵⁾ and Hideyuki Uyama⁵⁾

¹⁾ *International Research Center for Hydrogen Energy, Kyushu University, Fukuoka 819-0395, Japan*

²⁾ *Faculty of Engineering, Kyushu University, Fukuoka 819-0395, Japan*

³⁾ *Department of Mechanical Engineering, Kyushu University, Fukuoka 819-0395, Japan*

⁴⁾ *HYDROGENIUS, Kyushu University, Fukuoka 819-0395, Japan*

⁵⁾ *NSK Ltd., Kanagawa 251-8501, Japan*

¹⁾ yamabe.junichiro.575@m.kyushu-u.ac.jp

ABSTRACT

Hydrogen-entry properties of black oxide (BO)-treated and diamond-like carbon (DLC)-coated bearing steels, namely JIS-SUJ2, were investigated using high-pressure hydrogen gas. First, the hydrogen diffusivities of non-coated and palladium (Pd)-coated bearing steels were determined using cylindrical specimens. After exposing the specimens to hydrogen gas at a pressure of 100 MPa and a temperature of 85°C for 400 h, the hydrogen contents of the H-charged specimens were measured at constant temperatures in the range of 30–120°C using gas chromatography–mass spectroscopy. The hydrogen diffusivity was determined by fitting the solution of a diffusion equation to the experimental hydrogen contents measured at various constant temperatures. The hydrogen diffusivity of JIS-SUJ2 was approximately one order of magnitude lower than that of Cr–Mo steels. The temperature dependence of the hydrogen diffusivity of JIS-SUJ2 was successfully fitted using an Arrhenius-type equation. The activation energy of the hydrogen diffusivity was estimated to be 28 kJ/mol, which was approximately equal to that of the Cr–Mo steels. The following specimens were prepared from round bars of JIS-SUJ2: (1) non-coated, (2) BO-treated, (3) DLC-coated, and (4) Pd-coated specimens. After exposing the specimens to hydrogen gas at a pressure of 100 MPa and a temperature of 50°C for 27 h, the specimens were cut to 0.8-mm-thick samples. The hydrogen contents were then determined by increasing the temperature using quadrupole mass spectrometry. The results show that the hydrogen contents of the DLC-coated and Pd-coated samples were higher than the non-coated and BO-treated samples. The depth profiles of various elements obtained using Auger electron microscopy showed that the non-coated sample exhibited a native oxide layer with a

¹⁾ Research Professor

thickness of a few nanometers. An oxide layer was also formed in the BO-treated sample. However, the oxide layer was hardly observed on the surface of the DLC-coated sample. Moreover, the surface of the Pd-coated sample was covered with a Pd layer. A difference in the hydrogen contents between the samples is observed because the oxide layer in the surface inhibited the hydrogen dissociation. The experimental results show that the BO treatment and DLC coating failed to block the entry of hydrogen in a high-pressure hydrogen-gas environment.

1. INTRODUCTION

White structure flaking (WSF) is a type of premature failure observed in roller bearings (Evans 2012). It is well known that white etching areas are characteristic of WSF at a depth where the maximum shear stress is produced beneath a contact part of a roller bearing. The WSF is related to the hydrogen content in a material. Endo et al. (2004) conducted a rolling fatigue test wherein the hydrogen environment caused a significant degradation in the rolling fatigue life. Uyama et al. (2012) reported that the WSF was reproduced by rolling fatigue tests conducted on H-charged specimens. Based on these existing results, a model representing that the diffusible hydrogen generated in a tribochemical reaction of lubricants promotes the WSF has been proposed (Iso 2005). Because the hydrogen often degrades the tensile and fatigue properties of metals (Matsunaga 2015; Yamabe 2016), the hydrogen affects the WSF.

To prevent the WSF in rolling bearings, diamond-like carbon (DLC) coating is extensively applied to contact surfaces of the rolling bearing. Uyama et al. performed contact fatigue tests on non-coated and DLC-coated bearing steels under an environment wherein hydrogen is easily produced by decomposition of a lubricant. The results show that the WSF occurred in the non-coated steel, whereas it did not occur in the DLC-coated steel. This experimental result demonstrates that the DLC coating can be used to improve the resistance to the WSF. If the hydrogen produced by the decomposition of a lubricant affects the WSF, the DLC coating may have the capability to mitigate the hydrogen production or the hydrogen entry into the bearing steel. Among the influencing factors, it is difficult to directly analyze the hydrogen production. Hence, this study focuses on the hydrogen entry into a DLC-coated bearing steel.

Before identifying the resistance of the DLC coating to hydrogen entry, the hydrogen-diffusion properties of the bearing steel need to be determined. The hydrogen diffusivity of BCC steels is significantly affected by the lattice defects such as dislocations and vacancies (Kiuchi and McLellan 1983); hence, the hydrogen diffusivity should be identified in each steel. With regard to the hydrogen diffusivity of JIS-SUJ2, Matsubara and Hamada (2006) measured the hydrogen diffusivity at room temperature (RT) using an electrochemical permeation method; however, the temperature dependence of the hydrogen diffusivity in JIS-SUJ2 should be investigated in a practical environment.

This study focuses on the temperature dependence of the hydrogen diffusivity in a bearing steel, namely JIS-SUJ2, using a hydrogen-desorption method with high-pressure hydrogen gas (Matsuo et al. 2014; Yamabe et al. 2015). To analyze the resistance of the DLC coating to hydrogen entry, hydrogen-entry properties of JIS-

SUJ2 with various coatings (DLC, black oxide, and palladium) were also investigated under a high-pressure hydrogen-gas environment.

2. EXPERIMENTAL PROCEDURE

2.1 Material

The base steel used in this study is a bearing steel, namely JIS-SUJ2. Two bearing steels, namely SUJ2-A and SUJ2-B, were prepared. Table 1 presents the chemical compositions, heat-treatment conditions, and Vickers hardness values of the bearing steels. The chemical compositions and heat-treatment conditions of the steels were slightly different; however, the hydrogen-diffusion properties were assumed the same. Fig. 1 shows the microstructure of SUJ2-A using a scanning electron microscope (SEM). The microstructure shows a tempered martensitic structure.

Table 1 Chemical composition (mass %), heat-treatment condition, and Vickers hardness, HV^{*2} of JIS-SUJ2

Steel	C	Si	Mn	P	S	Cr	Quenching (°C)	Tempering (°C)	HV^{*2}
SUJ2-A	1.00	0.26	0.36	- ^{*1}	- ^{*1}	1.44	840	240	703
SUJ2-B	1.01	0.27	0.37	0.009	0.006	1.42	840	180	757

*1) Not measured, *2) Measured (10 points) with a load of 9.8 N.

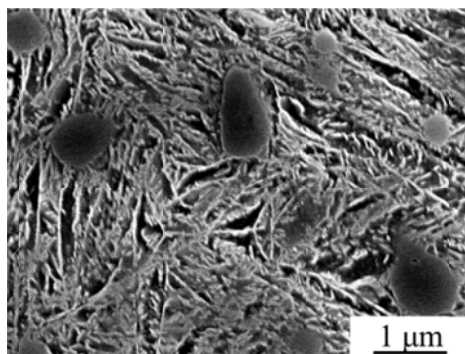


Fig. 1 SEM image of microstructure of SUJ2-A after etching with nital

2.2 Specimens

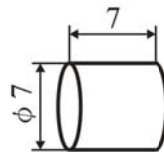
Fig. 2 shows the shapes and dimensions of the specimens. Fig. 2(a) shows the specimen made of SUJ2-A (specimen A) for determining the hydrogen diffusivity. For specimen A, $2r = z = 7$ mm, where r is the radius and z is the length. The surface was polished by a #1000 emery paper. After the polishing, the surfaces of some of the

specimens were coated with a 10-nm-thick palladium (Pd) layer. The Pd layer was coated to promote the hydrogen dissociation on the surface of the specimen.

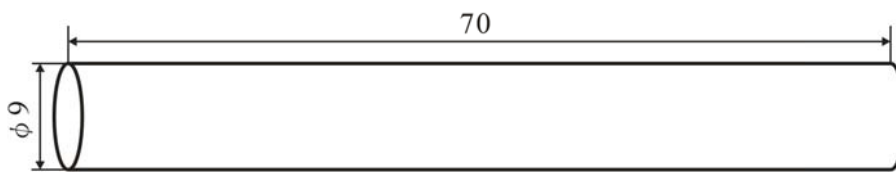
Fig. 2(b) shows the specimen for determining the hydrogen-entry property of coated steels (specimen B). For specimen B, $2r = 9$ mm and $z = 70$ mm. The circumferential surface of specimen B was coated with DLC, black oxide (BO), and Pd. The thicknesses of the coatings were $1.6 \mu\text{m}$ for the DLC coating and $1\text{--}2 \mu\text{m}$ for the BO treatment.

2.3 Determination of hydrogen diffusivity

Specimen A was exposed to hydrogen gas at a pressure of 100 MPa and a temperature of 85°C for 400 h. Preliminary investigations show that the specimens with different lengths exhibit the same hydrogen content under the present exposure condition. This indicates that the exposure to 100-MPa hydrogen gas at 85°C for 400 h leads to a uniform distribution of hydrogen. After the exposure, the hydrogen contents of the H-charged specimens were measured under constant temperatures (30 , 50 , 60 , 85 , and 120°C) using a gas chromatography–mass spectroscope (GC-MS). The hydrogen diffusivity was determined by fitting the solution of a diffusion equation to the experimental hydrogen contents measured at various constant temperatures (Demarez et al. 1954; Matsuo et al. 2014; Yamabe et al. 2015).



(a) Specimen A made of SUJ2-A



(b) Specimen B made of SUJ2-B

Fig. 2 Shapes and dimensions of specimens, in mm

2.4 Investigation of hydrogen entry of coated specimens

Specimens B with no coating, DLC coating, BO treatment, and Pd coating were exposed to hydrogen gas at a pressure of 100 MPa and a temperature of 50°C for 27 h. Based on the measured hydrogen diffusivity of JIS-SUJ2, shown in Fig. 4, the hydrogen content C_H was approximately equal to the saturated hydrogen content C_S ($C_H/C_S \approx 0.90$). After the exposure, the coated layers of the specimens were removed with a #1000 emery paper; subsequently, the specimens were cut to samples of thickness 0.8 mm. The hydrogen contents of the samples were then measured by increasing the temperature using a quadrupole mass spectrometer (QMS).

3. RESULTS AND DISCUSSION

3.1 Hydrogen diffusivity of JIS-SUJ2

Fig. 3 shows the Arrhenius plot of the hydrogen diffusivity for JIS-SUJ2. In addition, Fig. 3 shows the literature data for JIS-SUJ2 and low-alloy steels (Cr–Mo, Cr–Mo–V–W, and Ni–Cr–Mo steels) (Hobson 1958; Coe and Moreton 1966; Yamakawa et al. 1981; Kiuchi and McLellan 1983; Fujii 1984; Matsubara and Hamada 2006; Yamabe et al. 2015). The hydrogen desorption at approximately RT was significantly affected by the surface reaction of the hydrogen. To eliminate the surface reaction of hydrogen and realize the hydrogen-diffusion process, the hydrogen diffusivity at approximately RT was determined using the Pd-coated specimens. The results show that the hydrogen diffusivity of JIS-SUJ2 obtained in this study could be fitted using the Arrhenius-type equation. The extrapolated line of the measured hydrogen diffusivity at RT was consistent with the literature value obtained for JIS-SUJ2. In addition, the hydrogen diffusivity of JIS-SUJ2 was approximately one order of magnitude lower than that of Cr–Mo steels (Yamakawa 1981; Fujii and Nomura 1984; Yamabe et al. 2015).

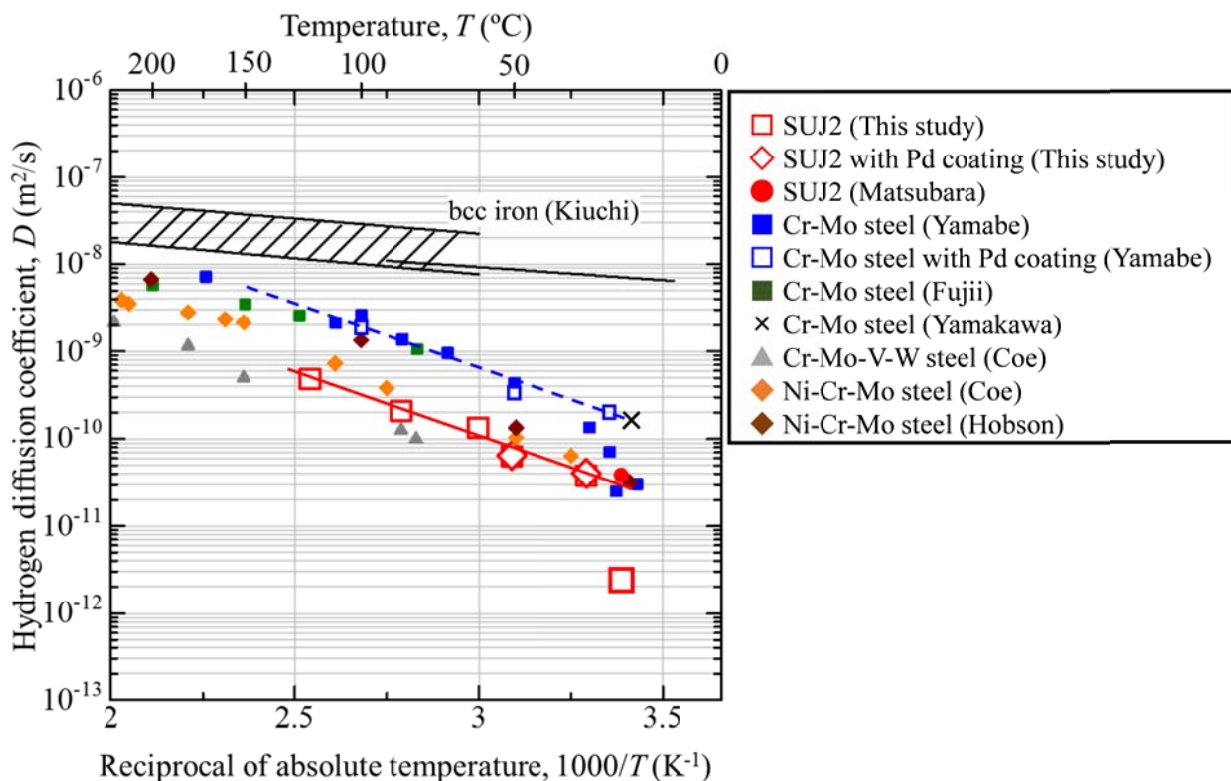


Fig. 3 Arrhenius plot of hydrogen diffusivity for JIS-SUJ2, along with literature data

The activation energy of the hydrogen diffusivity E_D for JIS-SUJ2 was approximately equal to that of the Cr–Mo steels, the value of which was estimated to be 28 kJ/mol. Accordingly, it is inferred that the hydrogen in both JIS-SUJ2 and Cr–Mo

steels was largely trapped by the elastic field of dislocations (Takai 2004; Novak et al. 2010; Yamabe et al. 2017), and the difference in the hydrogen diffusivities between JIS-SUJ2 and Cr–Mo steels was attributed to the difference in their dislocation densities.

3.2 Hydrogen-entry properties of JIS-SUJ2 with various coatings

Fig. 4 shows the hydrogen contents of non-coated, DLC-coated, BO-treated, and Pd-coated samples. Under the exposure to hydrogen gas at a pressure of 100 MPa and a temperature of 50°C for 27 h, the hydrogen contents of the H-charged samples were higher than that of the non-charged samples; moreover, the hydrogen entry occurred in the H-charged samples. Interestingly, the hydrogen contents of the H-charged samples with the coatings were in the following order: Pd-coated > DLC-coated > non-coated ≈ BO-treated samples. This implies that the DLC coating and BO treatment could not be used to block hydrogen entry under a high-pressure hydrogen-gas environment.

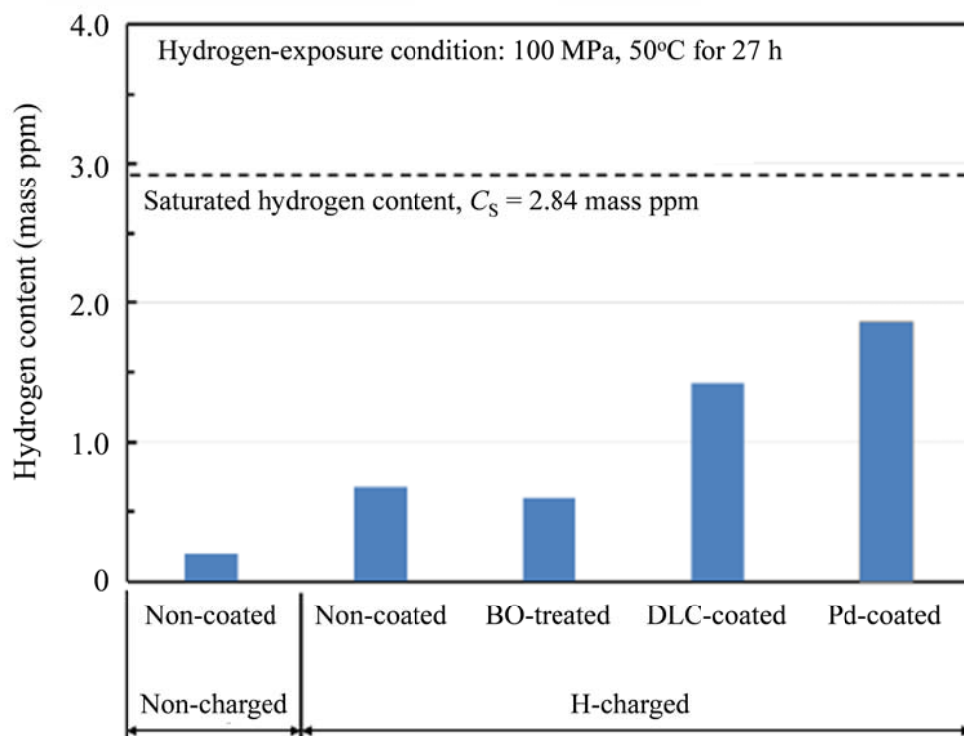


Fig. 4 Hydrogen-entry properties of JIS-SUJ2 with various coatings

Fig. 5 shows the depth profiles of various elements (O, C, Fe, Cr, Si, and Pd) of non-coated, DLC-coated, and Pd-coated samples identified using Auger electron microscopy (AEM). A native oxide layer with a thickness of ~4 nm was observed in the non-coated sample (Fig. 5(a)). The surface of the Pd-coated sample was covered with a Pd layer of thickness 10 nm, followed by a native oxide layer (Fig. 5(c)). The surface

of the BO-treated sample was also covered with an oxide layer with thicknesses in the range of 1–2 μm . This type of oxide layer was hardly observed on the surface of the DLC-coated sample (Fig. 5(b)). A series of experimental evidences suggest that the hydrogen entry in the samples was strongly related to the surface reaction of hydrogen under the present exposure condition, and the hydrogen entry was blocked via the inhibition of hydrogen dissociation.

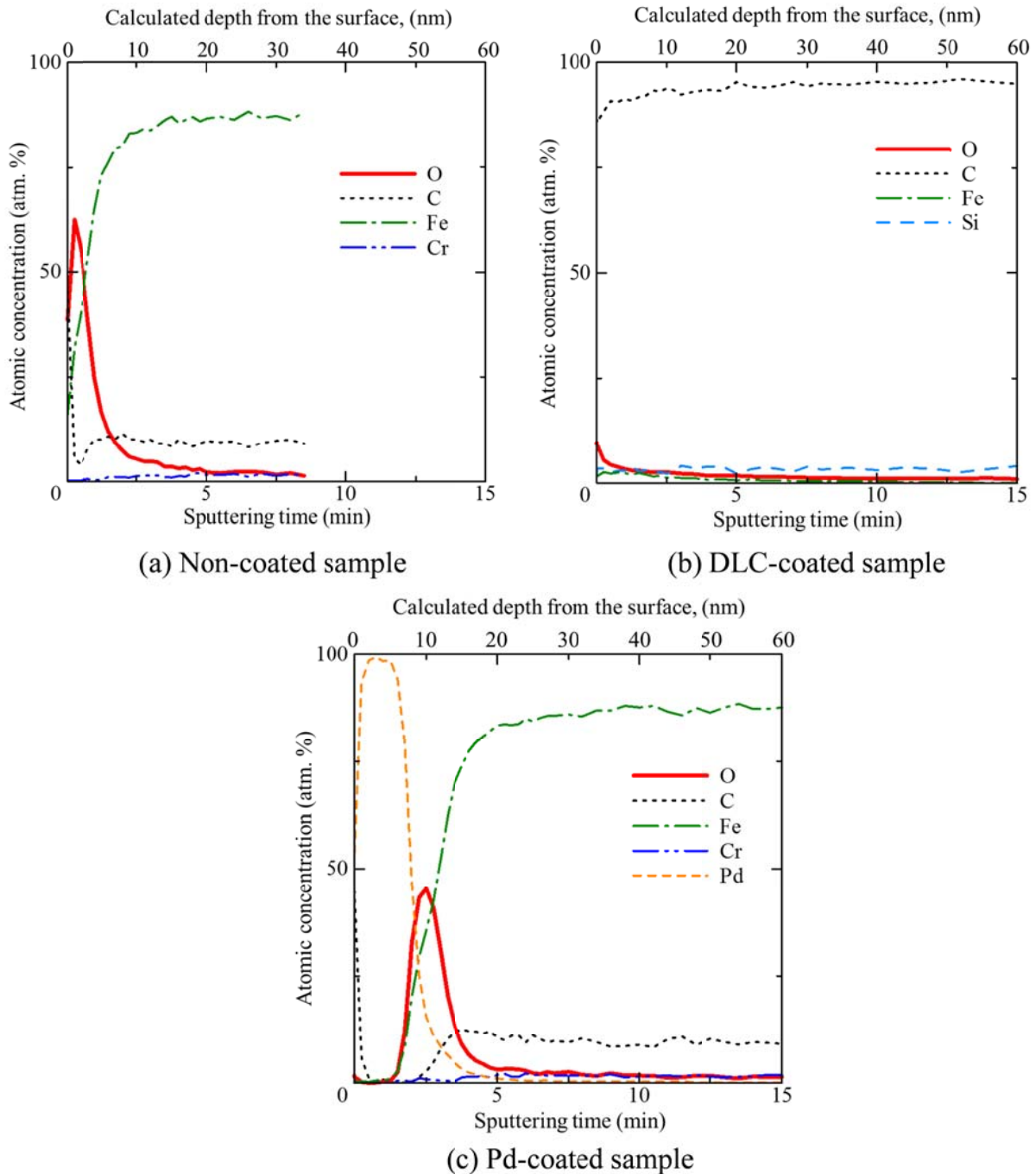


Fig. 5 Depth profiles of various elements obtained using AEM

Finally, it was interpreted that under the exposure to hydrogen gas at a pressure of 100 MPa and a temperature of 50°C for 27 h, the hydrogen entry in the Pd-coated samples occurred via the diffusion-controlled process, whereas the hydrogen entry in the other samples occurred via the surface reaction-controlled process. Nevertheless, the hydrogen content of the Pd-coated sample, shown in Fig. 5 ($C_H/C_S \approx 0.65$), was lower than that expected via the hydrogen diffusivity, shown in Fig. 4 ($C_H/C_S \approx 0.90$). This is because the trapping sites associated with non-diffusible hydrogen substantially affected the hydrogen diffusion in the Pd-coated sample, shown in Fig. 5. In fact, the ASTM G148 standard recommends performing multiple hydrogen permeation tests, preferably three permeation tests, to mitigate the effect of trapping sites associated with the non-diffusible hydrogen on the hydrogen permeation and obtain stable permeation curves. Moreover, we found that $C_H/C_S \approx 0.90$ for the second hydrogen-entry test conducted on the Pd-coated sample, wherein the effect of the trapping sites associated with the non-diffusible hydrogen was mitigated via the first hydrogen exposure. The rates of hydrogen entry and hydrogen desorption depend on the initial condition of hydrogen states.

4. CONCLUSIONS

This study investigated the hydrogen diffusivity of a bearing steel, namely JIS-SUJ2, and the effect of black oxide (BO) treatment and diamond-like carbon (DLC) coating on the hydrogen entry of JIS-SUJ2 under a high-pressure hydrogen-gas environment. As a reference, palladium (Pd) was coated on JIS-SUJ2 to promote hydrogen dissociation on the surface of the specimen. The conclusions of this study are summarized as follows:

- (1) The hydrogen diffusivity of JIS-SUJ2 could be fitted using the Arrhenius-type equation, showing one order of magnitude lower than that of Cr–Mo steels.
- (2) The activation energy of the hydrogen diffusivity E_D for JIS-SUJ2 was approximately equal to that of tempered Cr–Mo steels, where $E_D = 28$ kJ/mol. The hydrogen in both JIS-SUJ2 and Cr–Mo steels was largely trapped by the elastic field of the dislocations, and the difference in the hydrogen diffusivities between JIS-SUJ2 and Cr–Mo steels was attributed to the difference in their dislocation densities.
- (3) After the exposure to hydrogen gas at a pressure of 100 MPa and a temperature of 50°C for 27 h, the hydrogen contents in the coated samples were in the following order: Pd-coated > DLC-coated > non-coated \approx BO-treated samples. This reveals that the DLC coating and BO treatment could not be used to block hydrogen entry under the high-pressure hydrogen-gas environment.
- (4) The depth profiles of various elements measured using auger electron microscopy showed that the oxide layer was hardly observed on the surface of the DLC-coated sample, which is different from that observed in the non-coated and BO-treated samples. This infers that under the exposure to hydrogen gas at a pressure of 100 MPa and a temperature of 50°C for 27 h,

the hydrogen entry in the samples was strongly related to the surface reaction of hydrogen, and the hydrogen entry was blocked via the inhibition of hydrogen dissociation.

REFERENCES

- ASTM G148-97 (2011), "Standard practice for evaluation of hydrogen uptake, permeation, and transport in metals by an electrochemical technique."
- Coe, F.R. and Moreton, J. (1966), "Diffusion of hydrogen in low-alloy steel," *J. Iron. Steel. Inst. London*, **204**, 366–370.
- Demarez, A., Hock, A.G. and Meunier, F.A. (1954), "Diffusion of hydrogen in mild steel," *Acta Metall.*, **2**, 214–223.
- Endo, T., Dong, D., Imai, Y. and Yamamoto, Y. (2004), "Study on rolling contact fatigue in hydrogen atmosphere," *J. Jpn. Soc. Tribologists*, **49**, 801–808.
- Evans, M.-H. (2012), "White structure flaking (WSF) in wind turbine gearbox bearings: effects of 'butterflies' and white etching cracks (WECs)," *Mater. Sci. Technol.*, **28**, 3–22.
- Fujii, T. and Nomura, K. (1984), "Temperature dependence of hydrogen diffusivity of 2 1/4Cr-1Mo steel," *ISIJ Int.*, **70**, 104–111.
- Hobson, J.D. (1958), "The diffusivity of hydrogen in steel at temperatures of –78 to 200°C," *J. Iron. Steel. Inst. London*, **189**, 315–321.
- Iso, K., Yokouchi, A. and Takemura, H. (2005), "Research work for clarifying the mechanism of white structure flaking and extending the life of bearings," *SAE Technical Paper 2005-01-1868*, 12 pages.
- Kiuchi, K. and McLellan, R.B. (1983), "The solubility and diffusivity of hydrogen in well-annealed and deformed iron," *Acta Metall.*, **31**, 961–984.
- Matsubara, Y. and Hamada, H. (2006), "A novel method to evaluate the influence of hydrogen on fatigue properties of high strength steels," *J. ASTM Int.*, **3**, 1–13.
- Matsuo, T., Yamabe, J., Furukawa, H., Seki, K., Shimizu, K., Watanabe, S. and Matsuoka, S. (2014), "Development of new strain gage for high-pressure hydrogen gas use," *Exp. Mech.*, **54**, 431–442.
- Matsunaga, H., Yoshikawa, M., Kondo, R., Yamabe, J. and Matsuoka, S. (2015), "Slow strain rate tensile and fatigue properties of Cr-Mo and carbon steels in a 115 MPa hydrogen gas atmosphere," *Int. J. Hydrogen Energy*, **40**, 5734–5748.
- Novak, P., Yuan, R., Somerday, B.P., Sofronis, P. and Ritchie, R.O. (2010), "A statistical physical-based, micro-mechanical model of hydrogen-induced intergranular in steel," *J. Mech. Phys. Solids*, **58**, 206–226.
- Takai, K. (2004), "Hydrogen existing states in metals," *Trans. Jpn. Soc. Mech. Eng. A*, **70**, 1027–1035.
- Uyama, H., Yamada, H., Hidaka, H. and Mitamura, N. (2011), "The effect of hydrogen on microstructural change and surface originated flaking in rolling contact fatigue," *Tribology online*, **6**, 123–132.
- Yamabe, J., Awane, T. and Matsuoka, S. (2015), "Investigation of hydrogen transport behavior of various low-alloy steels with high-pressure hydrogen gas," *Int. J. Hydrogen Energy*, **40**, 11075–110861.

The 2017 World Congress on

Advances in Structural Engineering and Mechanics (ASEM17)

28 August - 1 September, 2017, Ilsan(Seoul), Korea

- Yamabe, J., Itoga, H., Awane, T., Matsuo, T., Matsunaga, H. and Matsuoka, S. (2016), "Pressure cycle testing of Cr-Mo steel pressure vessels subjected to gaseous hydrogen," *ASME J. Pres. Ves. Technol.*, **138**, 011401, 13 pages.
- Yamabe, J., Yoshikawa, M., Matsunaga, H. and Matsuoka, S. (2017), "Hydrogen trapping and fatigue crack growth property of low-carbon steel in hydrogen-gas environment," *Int. J. Fatigue*, **102**, 202–213.
- Yamakawa, K., Tsuruta, T. and Yoshizawa, S. (1981), "Interaction between dislocation and hydrogen occluded in single crystal of iron," *Boshoku Gijutsu*, **30**, 443–449.